

ARTICLE

Received 31 Mar 2016 | Accepted 4 Nov 2016 | Published 9 Jan 2017

DOI: 10.1038/ncomms13839

OPEN

The microbiota maintain homeostasis of liver-resident $\gamma\delta$ T-17 cells in a lipid antigen/CD1d-dependent manner

Fenglei Li¹, Xiaolei Hao², Yongyan Chen¹, Li Bai¹, Xiang Gao³, Zhexiong Lian¹, Haiming Wei^{1,2}, Rui Sun^{1,2,4} & Zhigang Tian^{1,2,4}

The microbiota control regional immunity using mechanisms such as inducing IL-17A-producing $\gamma\delta$ T ($\gamma\delta$ T-17) cells in various tissues. However, little is known regarding hepatic $\gamma\delta$ T cells that are constantly stimulated by gut commensal microbes. Here we show hepatic $\gamma\delta$ T cells are liver-resident cells and predominant producers of IL-17A. The microbiota sustain hepatic $\gamma\delta$ T-17 cell homeostasis, including activation, survival and proliferation. The global commensal quantity affects the number of liver-resident $\gamma\delta$ T-17 cells; indeed, *E. coli* alone can generate $\gamma\delta$ T-17 cells in a dose-dependent manner. Liver-resident $\gamma\delta$ T-17 cell homeostasis depends on hepatocyte-expressed CD1d, that present lipid antigen, but not Toll-like receptors or IL-1/IL-23 receptor signalling. Supplementing mice *in vivo* or loading hepatocytes *in vitro* with exogenous commensal lipid antigens augments the hepatic $\gamma\delta$ T-17 cell number. Moreover, the microbiota accelerate nonalcoholic fatty liver disease through hepatic $\gamma\delta$ T-17 cells. Thus, our work describes a unique liver-resident $\gamma\delta$ T-17 cell subset maintained by gut commensal microbes through CD1d/lipid antigens.

¹Institute of Immunology and the Key Laboratory of Innate Immunity and Chronic Disease (Chinese Academy of Science), School of Life Science and Medical Center, University of Science and Technology of China, Hefei 230027, China. ²Hefei National Laboratory for Physical Sciences at Microscale, Hefei, Anhui 230027, China. ³Model Animal Research Center, Nanjing University, Nanjing, Jiangsu 210061, China. ⁴Collaborative Innovation Center for Diagnosis and Treatment of Infectious Diseases, State Key Laboratory for Diagnosis and Treatment of Infectious Diseases, First Affiliated Hospital, College of Medicine, Zhejiang University, Hangzhou, Zhejiang 310003, China. Correspondence and requests for materials should be addressed to Z.T. (email: tzg@ustc.edu.cn).

The liver is situated in a unique systemic circulation system that receives blood from both the hepatic artery and the portal vein, making this organ a prime location for both metabolic and immune function^{1–3}. However, the precise mechanism that connects the microbiota and the hepatic immune response is seldom reported. Bacterial translocation and pathogen-associated molecular pattern (PAMP) transport are the two main events that have been observed in the liver–gut axis^{4,5}. However, the proposed mechanisms will remain elusive until the soluble factors from the microbiota and their cellular targets in liver–gut axis are determined.

The liver is enriched in innate immune cells, including $\gamma\delta$ T cells at a frequency of 3–5% (5 to 10-fold greater than in other tissues or organs) within total liver lymphocytes¹. $\gamma\delta$ T cells function as a bridge between innate and adaptive immunity because they express a rearranged T-cell receptor (TCR) that recognizes certain antigens and can also rapidly secrete pro-inflammatory cytokines including interleukin (IL)-17A upon stimulation⁶. By producing IL-17A to recruit neutrophils and enhance adaptive immunity, IL-17A-producing $\gamma\delta$ T ($\gamma\delta$ T-17) cells have an important role in host defence against bacterial, fungal and viral infections, as well as stress, tumour surveillance and auto-immune diseases⁷. However, although hepatic $\gamma\delta$ T cells are involved in several liver immune diseases⁸, their physiological characteristics, and why the liver contains such high levels of $\gamma\delta$ T cells, are unknown.

CD1d, a typical lipid presentation molecule for natural killer T (NKT) cells⁹, can also present lipid antigens to the $\gamma\delta$ TCR and activate $\gamma\delta$ T cells¹⁰. A $\gamma\delta$ T cell subset in human blood can respond to CD1d-presented sulfatide, a lipid antigen present in both hosts and bacteria¹¹. Another $\gamma\delta$ T cell subset in the mouse duodenum can respond to exogenous lipid antigens including phosphatidylcholine, phosphatidylethanolamine (PE) and phosphatidylglycerol (PG) presented by CD1d¹². The liver constantly encounters microbial lipid components, and crosstalk occurs between CD1d and liver NKT cells^{13–16}; however, little is known regarding the role of $\gamma\delta$ T cells in this process.

Here we compare $\gamma\delta$ T cells originating from several organs and identify a liver-resident $\gamma\delta$ T-cell population that predominantly produces IL-17A. The microbiota maintain hepatic $\gamma\delta$ T-17 cell homeostasis, the underlying mechanism of which involves microbiota lipid antigens presented by hepatocyte-expressed CD1d, but not PAMPs or cytokine signals. Moreover, liver-resident $\gamma\delta$ T cells responding to the microbiota contribute to nonalcoholic fatty liver disease (NAFLD).

Results

Hepatic $\gamma\delta$ T cells produce IL-17A. Compared with other immune organs and tissues, hepatic $\gamma\delta$ T cells predominantly produced high levels of IL-17A, similar to $\gamma\delta$ T cells from the peritoneal cavity (PC) and lung and significantly higher than those from inguinal lymph nodes (iLNs), the spleen, the thymus, small intestine intraepithelial lymphocytes (IEL), colon IEL and mesenteric LN (mLN) (Fig. 1a,c). In terms of phenotype, hepatic $\gamma\delta$ T cells exhibited mixed V γ chain usage, which was also distinct from $\gamma\delta$ T cells of other organs (Fig. 1b). They were in a more active and mature state, as indicated by higher percentages of CD44^{high}CD62L[–] cells and lower CD24 expression (Fig. 1c). Corresponding with their high IL-17A expression levels, hepatic $\gamma\delta$ T cells expressed low levels of CD27 (Fig. 1c), which is a fate determinant of $\gamma\delta$ T cells to express IFN- γ ($\gamma\delta$ T-1) but not IL-17A ($\gamma\delta$ T-17)¹⁷. However, unlike $\gamma\delta$ T cells of the PC and lung, hepatic $\gamma\delta$ T cells rarely expressed cytokine receptors including CD121, CD25 and CD127 (Fig. 1c). Interestingly, neonatal mice had low levels of $\gamma\delta$ T-17 but high levels of $\gamma\delta$ T-1 cells in the liver

(Fig. 1d). As the mice aged, the hepatic $\gamma\delta$ T-17 cell frequency increased, while that of $\gamma\delta$ T-1 cells decreased, suggesting that hepatic $\gamma\delta$ T-17 cells might be induced after birth (Fig. 1d). Overall, hepatic $\gamma\delta$ T cells exhibited a unique composition and phenotype, indicating that they represent a distinct $\gamma\delta$ T-cell subtype.

We further characterized the trafficking and homing tendencies of hepatic $\gamma\delta$ T cells. GFP⁺ splenic and CD45.1⁺ hepatic lymphocytes were transferred separately or together into *Cd45.2⁺ Tcrd^{-/-}* mice (Supplementary Fig. 1a). One day after transfer, splenic $\gamma\delta$ T cells travelled randomly into both the spleens and the livers of recipient mice. In contrast, hepatic $\gamma\delta$ T cells selectively homed only to the liver, and co-transfer with splenic lymphocytes did not change this homing tendency. We confirmed this result by transferring purified hepatic $\gamma\delta$ T cells into *Rag1^{-/-}* mice and found that hepatic $\gamma\delta$ T cells, particularly $\gamma\delta$ T-17 cells, homed back to the liver but not to other organs (Supplementary Fig. 1b). To further explore whether hepatic $\gamma\delta$ T cells reside in the liver, CD45-congenic mice were surgically joined by parabiosis and evaluated for chimerism in various cell populations 2 weeks later. While conventional T cells exhibited substantial chimerism (Fig. 1e), the livers of CD45.1 parabiont mice contained almost all CD45.1⁺ $\gamma\delta$ T cells with very few, if any, CD45.2⁺ $\gamma\delta$ T cells; vice versa was observed in CD45.2 parabiont mice (Fig. 1e). Interestingly, PC and thymic $\gamma\delta$ T cells were also locally retained, but lung, spleen and iLN $\gamma\delta$ T cells were mutually exchanged (Supplementary Fig. 1c).

Compared with circulating $\gamma\delta$ T cells, most of the chemokine receptors and integrin molecules were expressed at lower levels on hepatic $\gamma\delta$ T cells, but C-X-C chemokine receptor 6 (CXCR6) was expressed at extremely high levels on hepatic $\gamma\delta$ T cells (Supplementary Fig. 2a). However, it was not involved in the liver homing of hepatic $\gamma\delta$ T cells because the numbers of hepatic $\gamma\delta$ T cells and $\gamma\delta$ T-17 cells were not changed in *Cxcr6^{-/-}* mice (Supplementary Fig. 2b), although CXCR6 was important for the liver homing of natural killer (NK) and NKT cells^{18,19}. Moreover, the liver residency of hepatic $\gamma\delta$ T cells was absent in *Il17a^{-/-}* mice. WT and *Il17a^{-/-}* mice were surgically joined by parabiosis; 2 weeks later, the WT mouse liver contained few *Il17a^{-/-}* mouse-derived $\gamma\delta$ T cells, but the *Il17a^{-/-}* mouse liver contained nearly 50% $\gamma\delta$ T cells derived from the WT mouse (Supplementary Fig. 2c). These results suggest that $\gamma\delta$ T cell liver homing might be related to their IL-17 expression ability in unknown mechanism.

In summary, these data collectively indicate that liver-resident $\gamma\delta$ T cells are indeed a unique $\gamma\delta$ T-cell subset with low expression levels of cytokine receptors, and that predominantly produce high levels of IL-17A and are retained in the liver.

The microbiota maintain hepatic $\gamma\delta$ T-17 cell homeostasis. To explore if the microbiota might influence liver-resident $\gamma\delta$ T-17 cells, antibiotics were used to clear mouse gut bacteria as previously reported²⁰. The antibiotic (Abx)-treated mice had a sharp decrease in commensal microbes, as indicated by the 99% reduction in cultivable bacteria, 95% reduction in bacterial DNA and elongated caecum (Supplementary Fig. 3a–c). Moreover, Abx-treated mice displayed a normal peripheral immune response (Supplementary Fig. 3d). Although the total number and frequency of hepatic B, T, NK, NKT and regulatory T (Treg) cells were normal in Abx-treated mice (Supplementary Fig. 3e,f), the accumulation of liver-resident $\gamma\delta$ T-17 cells during ontogeny was blocked in mice treated with antibiotics beginning *in utero* through the pregnant mother (Fig. 2a). The reduction in CD27 expression on hepatic $\gamma\delta$ T cells was also arrested, but the decline of hepatic $\gamma\delta$ T-1 cells was not affected (Fig. 2a).

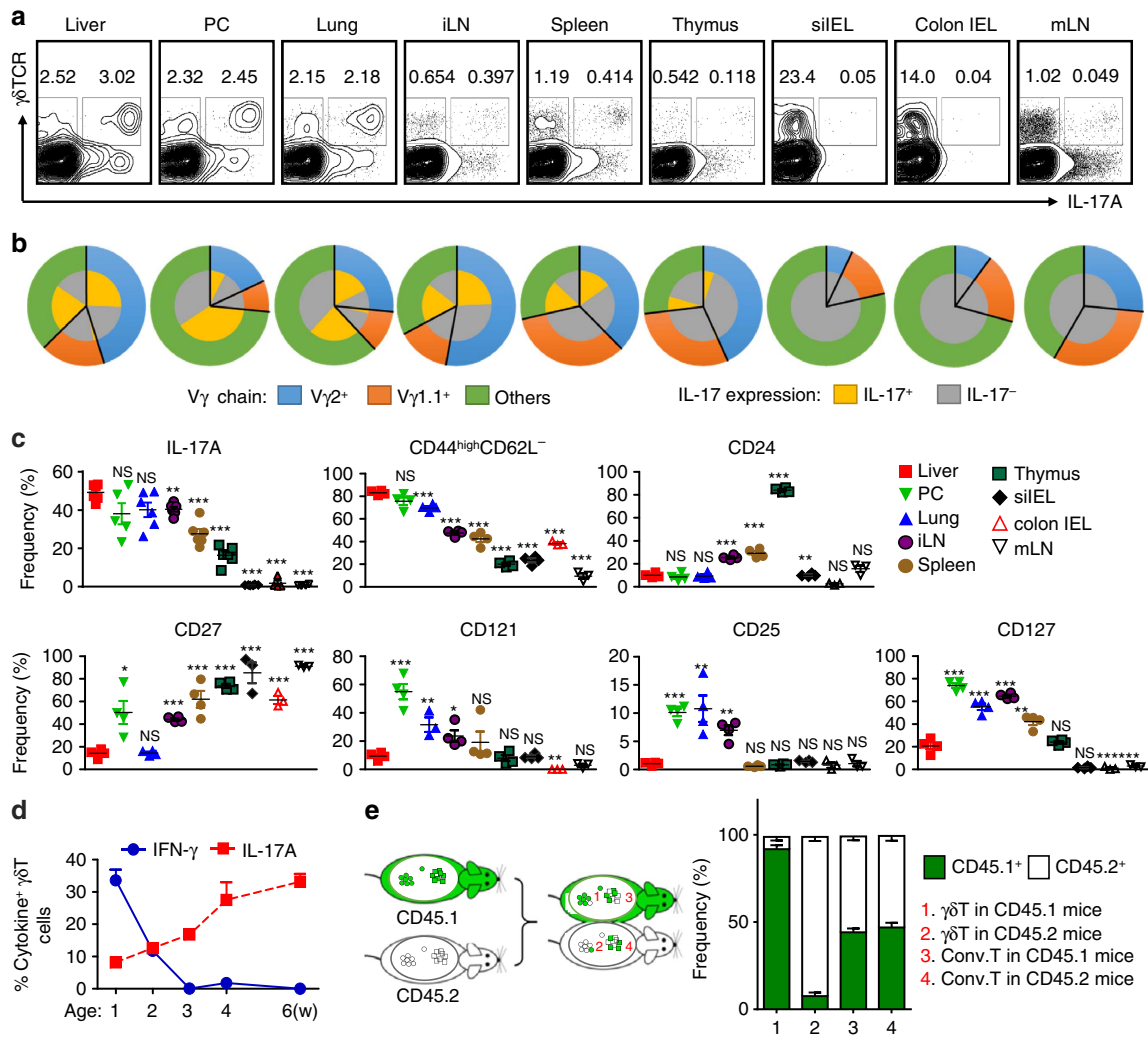


Figure 1 | Hepatic $\gamma\delta$ T-17 cells are major $\gamma\delta$ T population and liver-resident in adults. (a) FACS analysis of IL-17A expression by PMA/ionomycin-stimulated $\gamma\delta$ T cells from the indicated organs of B6 mice, gated on CD3⁺ T cells. (b) FACS analysis of V γ chain usage and IL-17A expression by each $\gamma\delta$ T-cell subtype. (c) Frequency of $\gamma\delta$ T cells expressing the indicated markers; each dot represents a mouse. (d) IFN- γ and IL-17A expression by hepatic $\gamma\delta$ T cells at the indicated B6 mouse age over time ($n=5$ /time point). (e) The host origin (CD45.1⁺ or CD45.2⁺) of hepatic $\gamma\delta$ T (CD3⁺TCR $\gamma\delta$ ⁺) and conventional T (CD3⁺TCR $\gamma\delta$ ⁻ NK1.1⁻) cells was identified by FACS analysis in each mouse of CD45.1/CD45.2 parabiotic B6 mouse pairs at 14 days post surgery ($n=5$ pairs). The data are representative of three independent experiments. The mean \pm s.e.m. is shown. (* $P<0.05$; ** $P<0.01$; *** $P<0.001$. one-way ANOVA with post hoc test). IEL, intraepithelial lymphocyte; iLN, inguinal lymph node; mLN, mesenteric lymph node; PC, peritoneal cavity; si, small intestine.

To directly observe the interaction between hepatic $\gamma\delta$ T-17 cells and the microbiota, germ-free (GF) mice were used, which had even more significantly decreased numbers of hepatic $\gamma\delta$ T-17 cells than Abx-treated SPF mice (Fig. 2b). In addition, treating GF mice with antibiotics did not further reduce their hepatic $\gamma\delta$ T-17 cell numbers, suggesting that antibiotics were not directly toxic to $\gamma\delta$ T-17 cells (Fig. 2b). Reconstituting Abx-treated mice with gut commensal microbes was sufficient to restore their reduced hepatic $\gamma\delta$ T-17 cell numbers to a normal level (Fig. 2b). The kinetics of hepatic $\gamma\delta$ T-17 cell recovery in commensal microbe-reconstituted GF mice were also studied. Commensal microbe reconstitution recovered the hepatic $\gamma\delta$ T-17 cell number gradually, reaching a similar level to that in SPF mice after 4 weeks of reconstruction (Fig. 2c). These results indicate that the accumulation of hepatic $\gamma\delta$ T cells relies on microbiotas.

The reduced hepatic $\gamma\delta$ T-17 cells in Abx-treated mice and GF mice were not restricted by V γ chain usage (Fig. 2d). Consistent with the reduced IL-17A expression by $\gamma\delta$ T cells from Abx-treated mice and GF mice, they were less diffe-

ntiated and less activated, as indicated by the lower proportions of CD27⁻CCR6⁺ and CD44^{high}CD62L⁻ cells (Fig. 2e). Moreover, enhanced apoptosis and reduced proliferation of hepatic $\gamma\delta$ T cells were also observed after Abx treatment (Fig. 2e). To better understand the specific influence of the microbiota on hepatic lymphocytes, an *in vivo* BrdU incorporation method was used to assay the cell proliferation. Only $\gamma\delta$ T-17 cells, but not NK, $\alpha\beta$ T or even IL-17A-negative $\gamma\delta$ T cells, displayed reduced BrdU incorporation and Ki67 expression in Abx-treated mice, indicating that the microbiota specifically promoted the proliferation of hepatic $\gamma\delta$ T-17 cells, but not all lymphocytes, in the liver (Fig. 2f). Together, these data indicated that the microbiota sustain liver-resident $\gamma\delta$ T-17 cell homeostasis by maintaining their normal activation, survival and proliferation.

Global commensal load affects hepatic $\gamma\delta$ T-17 cell number. To screen for bacteria that influence liver-resident $\gamma\delta$ T-17 cell numbers, different combinations of antibiotics (A, ampicillin; V,

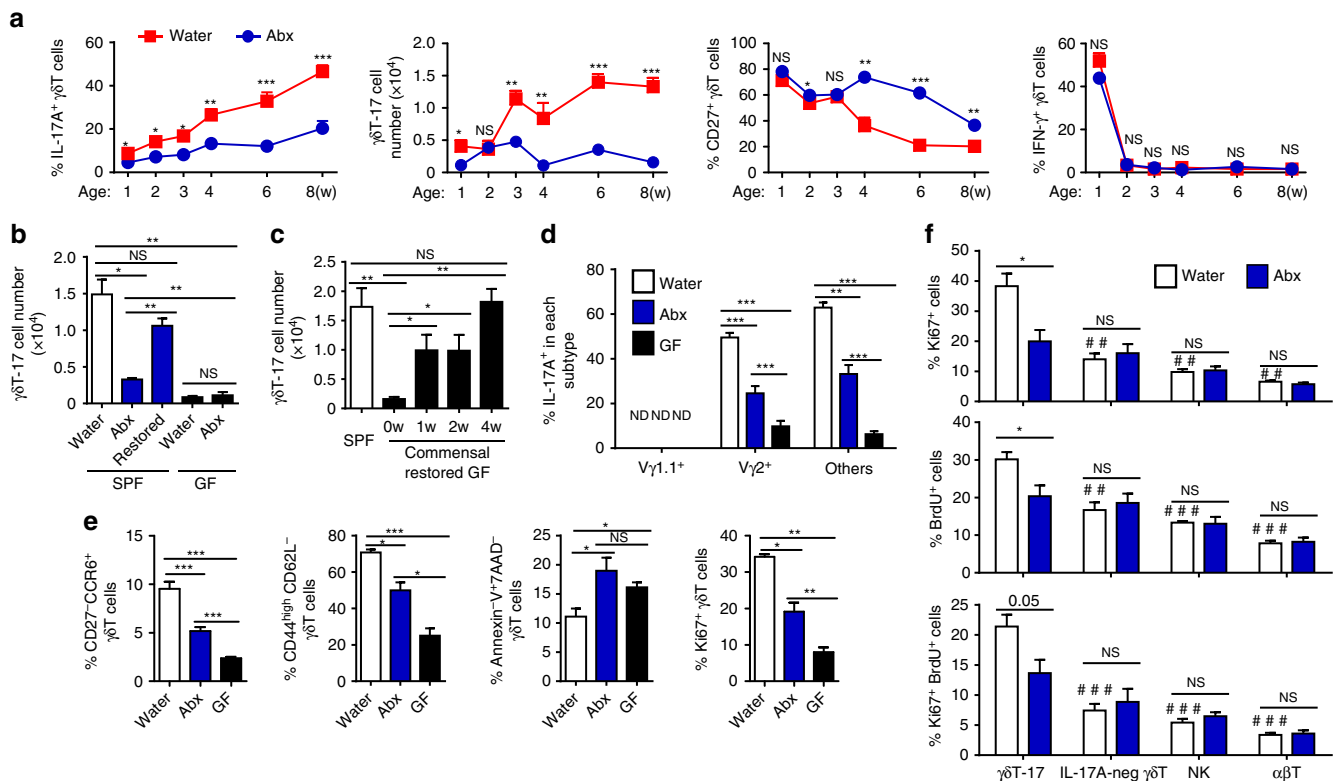


Figure 2 | The microbiota maintain the pool of hepatic $\gamma\delta$ T-17 cells in steady state. (a) FACS analysis of IL-17A, CD27 and IFN- γ expression by hepatic $\gamma\delta$ T cells at the indicated B6 mouse ages over time. The mice began treatment with water alone (Water) or containing antibiotics (Abx) *in utero* through the pregnant mother ($n = 7$ /time point). (b) Five-week-old adult SPF B6 mice and GF mice were fed water alone (Water) or containing antibiotics (Abx) for 4 weeks. Abx-pretreated SPF mice were co-housed with normal mice for an additional 4 weeks to reconstitute their gut bacteria (Restored), and the hepatic $\gamma\delta$ T-17 cell numbers were evaluated by FACS ($n = 4$ for SPF mice, $n = 5$ for GF mice). (c) Ten-week-old GF mice were co-housed with SPF mice to restore their commensal microbes, and the hepatic $\gamma\delta$ T-cell number was detected at the indicated time points post co-housing ($n = 9, 4, 5, 10$; from left to right). The frequency of IL-17A expression by each hepatic $\gamma\delta$ T-cell subtype ($n = 10, 7, 5$; from top to bottom) (d) and the frequency of hepatic $\gamma\delta$ T cells with the phenotype CD44^{high}CD62L⁻, CD27⁻CCR6⁺, Annexin-V⁺7AAD⁻ and Ki67⁺ ($n = 5$ per group) (e) from Water-treated mice, Abx-treated mice and GF mice were analysed by FACS. (f) Control and Abx-treated mice were i.p. injected with 1 mg BrdU three times at 2-day intervals, and BrdU incorporation and Ki67 expression by hepatic $\gamma\delta$ T-17 (CD3⁺ $\gamma\delta$ TCR⁺IL-17⁺), IL-17A negative $\gamma\delta$ T (CD3⁺ $\gamma\delta$ TCR⁺IL-17⁻), NK (CD3⁺NK1.1⁺) and $\alpha\beta$ T (CD3⁺TCR β ⁺) cells were evaluated by FACS. Differences between $\gamma\delta$ T-17 cells and other cells from control mice (indicated as '#') and differences between Water- and Abx-treated mice of each subtype of cells (indicated as '**') are shown ($n = 6, 4$; Water, Abx). The data are representative of more than three independent experiments. The mean \pm s.e.m. is shown (* $P < 0.05$; ** $##P < 0.01$; *** $###P < 0.001$ one-way ANOVA with post hoc test.).

vancomycin; N, neomycin; M, metronidazole) were used to treat mice. Different antibiotic mixtures had different targets (Supplementary Fig. 4a,b); thus, we produced a series of mice with commensal microbes at various clusters (Supplementary Fig. 4c) and diversities (Supplementary Fig. 4d). However, although different compositions of microbes were induced in the mice (Fig. 3a), there was almost no correlation between the $\gamma\delta$ T-17 cell number and the antibiotic type (Fig. 3b) or the bacteria species diversity (Fig. 3c).

Interestingly, the mice with low levels of microbes always had small numbers of hepatic $\gamma\delta$ T-17 cells, and the mice with high levels of microbes always had large numbers of hepatic $\gamma\delta$ T-17 cells (Fig. 3b). Indeed, both the numbers and the proliferation percentages of hepatic $\gamma\delta$ T-17 cells positively correlated with the global microbe DNA loads (Fig. 3d). These results suggest that the global bacterial load is a key factor in the homeostasis of liver-resident $\gamma\delta$ T-17 cells.

E. coli, a typical type of commensal microbe, was chosen to further explore this hypothesis. *E. coli* was completely deleted in eight groups of mice, including the A, V, AM, VN, AVM, AVN, VNM and AVNM groups (Fig. 4a), but some mice without *E. coli* (V, AVM and AVN groups) still had a comparable level of hepatic $\gamma\delta$ T-17 cells as normal mice (Fig. 3b), suggesting that

E. coli is not an irreplaceable bacterium for liver-resident $\gamma\delta$ T-17 cell homeostasis; indeed, there was no correlation with $\gamma\delta$ T-17 cell numbers (Fig. 4b). However, similar to the transfer of fresh faeces, transferring *E. coli* alone recovered the decline in hepatic $\gamma\delta$ T-17 cells in Abx-treated mice, with dose dependency in single *E. coli*-transferred mice (Fig. 4c). Thus, these results indicate that the global bacterial load, regardless of species specificity, is important for hepatic $\gamma\delta$ T-17 cell homeostasis.

CD1d presents commensal lipid antigen to hepatic $\gamma\delta$ T-17 cell.

To investigate the mechanism by which the microbiota/*E. coli* promote liver-resident $\gamma\delta$ T-17 cell accumulation, microbiota-derived PAMPs were evaluated. Though TLR agonists, such as poly(I:C) (a TLR3 ligand), could increase the hepatic $\gamma\delta$ T-17 cell number in WT mice (Supplementary Fig. 5a), administration of Pam3Csk4 (a TLR1/2 ligand), LPS (a TLR4 ligand), CpG (a TLR9 ligand), curdlan (a Dectin-1 ligand) or poly(I:C) could not restore hepatic $\gamma\delta$ T-17 cells in Abx-treated mice (Supplementary Fig. 5b,c). Moreover, TLR2/TLR4/TLR9 deficiency did not influence hepatic $\gamma\delta$ T-17 cells (Supplementary Fig. 5d). The second microbiota-associated candidate for regulating hepatic $\gamma\delta$ T-17 cells was cytokine signalling. However, the levels of liver cytokines (Supplementary Fig. 5e) and the cytokine receptor

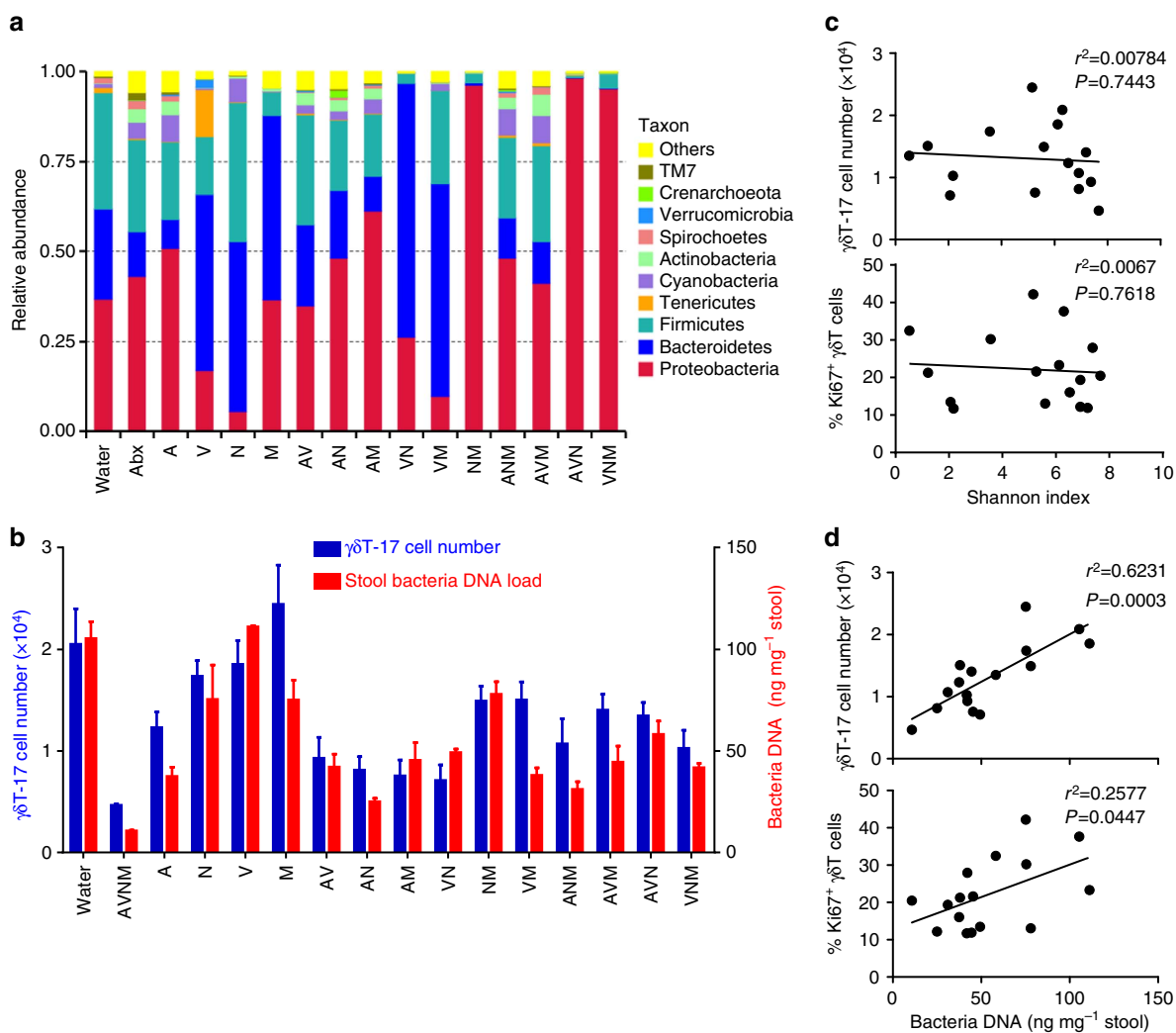


Figure 3 | Commensal microbe load is positively correlated with hepatic $\gamma\delta T-17$ cell numbers. Mice were fed for 4 weeks with water alone (Water) or containing the following antibiotics for 4 weeks (A = ampicillin; V = vancomycin; N = neomycin; M = metronidazole): all four (AVNM), each one alone or in various combinations (AV, AN, AM, VN, VM, NM, AVN, AVM, VNM and ANM). **(a)** Genomic bacterial DNA was isolated from faecal samples, and the V5–V6 hypervariable region of 16S rDNA was amplified and sequenced. The average percentages of reads for the three experimental groups are shown. **(b)** The left axis indicates the number of hepatic $\gamma\delta T-17$ cells determined by FACS, and the right axis indicates the DNA load of bacteria in the faeces. **(c)** The Shannon index of diversity relative to species was calculated, and Pearson correlation curves with the $\gamma\delta T-17$ cell number and Ki67 expression are shown. **(d)** The Pearson correlation curves between the $\gamma\delta T-17$ cell number and Ki67 expression with the bacterial DNA load. The data are representative of more than three independent experiments ($n=7$ mice per group). Either a representative plot or the mean \pm s.e.m. is shown.

expressions on hepatic $\gamma\delta T$ cells (Supplementary Fig. 5f) were unchanged in Abx-treated mice, though CD121 expression on PC $\gamma\delta T$ cells was reduced (Supplementary Fig. 5f), as previously reported²¹. Neutralizing antibodies against IL-1 β and IL-23 *in vivo* reduced the number of PC $\gamma\delta T-17$ cells, but not hepatic $\gamma\delta T-17$ cells (Supplementary Fig. 5g). Thus, PAMPs and cytokine signals do not support the homeostasis of liver-resident $\gamma\delta T-17$ cells.

The liver is rich in lipid antigens and CD1d; thus, we speculated that CD1d/lipid antigen complexes interact with liver-resident $\gamma\delta T-17$ cells in the liver. WT and *Cd1d*^{-/-} mice were co-housed to share the same microbiota, but *Cd1d*^{-/-} mice had a decreased number of hepatic $\gamma\delta T-17$ cells with lower proportions of CD27⁻CCR6⁺ cells compared with WT mice, similar to the result observed in Abx-treated WT mice (Fig. 5a). Co-housed NKT-deficient *Ja18*^{-/-} mice had similar hepatic $\gamma\delta T-17$ cell numbers to WT mice, demonstrating that CD1d sustained hepatic $\gamma\delta T-17$ cells directly and independently of NKT cells (Fig. 5b). Moreover, Abx-treatment did not further

downregulate the number and frequency of hepatic $\gamma\delta T-17$ cells in *Cd1d*^{-/-} mice (Fig. 5a). Collectively, these data indicate that the microbiota maintain the homeostasis of liver-resident $\gamma\delta T-17$ cells mainly through CD1d signalling.

To explore whether CD1d-associated lipid antigens indeed have a role in this process, Abx-treated WT mice were injected with previously reported CD1d-presenting bacterial lipid antigens, including *E. coli* cardiolipin (CL), PG, PE and total polar lipid extract from *E. coli*. After receiving exogenous *E. coli*-derived lipids, the liver-resident $\gamma\delta T-17$ cell number, proliferation and CD27⁻CCR6⁺ expression levels partially but markedly recovered in Abx-treated WT mice but not in *Cd1d*^{-/-} mice (Fig. 5c), indicating that lipid antigens act in a CD1d-dependent manner. Moreover, lipid antigens still induced the recovery of the hepatic $\gamma\delta T-17$ cell numbers in Abx-treated IL-1/IL-23-neutralized mice (Supplementary Fig. 5h) and TLR2/TLR4/TLR9-deficient mice (Supplementary Fig. 5i), which further suggested that lipid antigens maintain the pool of liver-resident $\gamma\delta T-17$ cells in a TLR/cytokine signal-independent manner.

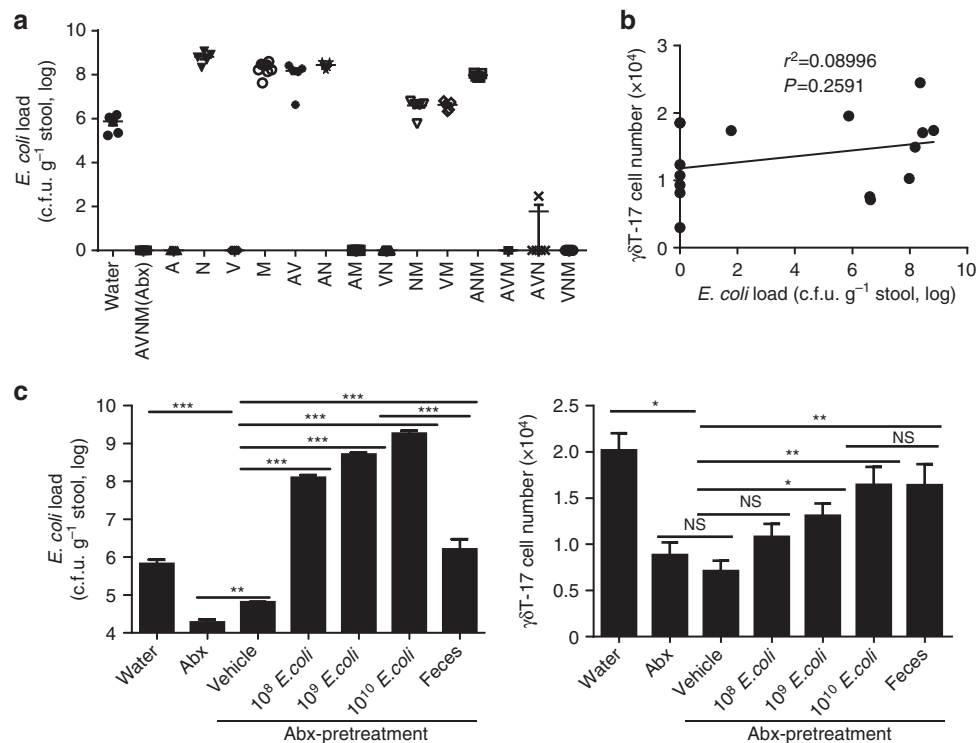


Figure 4 | *E. coli* is sufficient but not essential to promote hepatic $\gamma\delta T-17$ cells. Mice were treated with antibiotics as described in Fig. 3. **(a)** *E. coli* in fresh stool were plated and counted on an EMB plate (each dot represents a mouse). **(b)** The Pearson correlation curve between the $\gamma\delta T-17$ cell number and the *E. coli* load. **(c)** Abx-pretreated mice continued on Abx (Abx) or untreated (Abx-pretreatment) water, and then the Abx-pretreated mice were intragastrically administered vehicle, 10^8 c.f.u. *E. coli*, 10^9 c.f.u. *E. coli*, 10^{10} c.f.u. *E. coli* or 10 mg fresh faeces (Faeces). *E. coli* and faeces were from normal mice. The stool *E. coli* load (3 days post transfer) and hepatic $\gamma\delta T-17$ cell numbers (3 weeks post transfer) were detected ($n = 5, 6, 6, 6, 8, 7$; from left to right). The data are representative of three independent experiments. The mean \pm s.e.m. is shown (* $P < 0.05$; ** $P < 0.01$ one-way ANOVA with post hoc test).

Some microbiota metabolic molecules may reach the liver via the portal vein²². To explore if microbiota lipid antigens could reach the liver, ¹⁴C-glucose was used to label *E. coli* that was then intragastrically delivered into mice. After 6h, there was high radioactivity in the lipids extracted from the livers of mice transferred with ¹⁴C-glucose labelled *E. coli* but not in the mice transferred with unlabelled *E. coli* (Fig. 5d). This suggest that microbial lipids can enter the liver at steady state, which allows them to encounter hepatic $\gamma\delta T-17$ cells in the liver. $\gamma\delta T-17$ cells from both the liver and the spleen were stained with CD1d tetramers loaded with different lipid antigens (PE, PG, CL and PBS57), and liver, but not spleen, $\gamma\delta T-17$ cells specifically recognized *E. coli*-derived lipid antigens (PE, PG and CL) and a model antigen PBS57 (ref. 23; Fig. 5e). In addition, these CD1d tetramer-positive $\gamma\delta T-17$ cells in the liver decreased markedly after microbiota depletion (Fig. 5f). These results indicate that liver $\gamma\delta T-17$ cells specifically recognize microbiota-derived lipid antigens.

Next, we asked which cells expressed CD1d stimulate hepatic $\gamma\delta T-17$ cells. Using fetal liver chimeric mice, we found that the number of hepatic $\gamma\delta T-17$ cells decreased only when CD1d was deficient in non-hematopoietic cells, but not in hematopoietic cells (Fig. 6a). Indeed, when using clodronate to deplete macrophages and dendritic cells (DCs), both of which are major hematopoietic cells expressing CD1d, the number of hepatic $\gamma\delta T-17$ cells was not reduced but rather slightly increased (Fig. 6b). Interestingly, the hepatocytes expressed a high level of CD1d (Fig. 6c), as previously reported²⁴. In the *in vitro* co-culture system, WT hepatocytes displayed a higher ability to promote $\gamma\delta T-17$ cells than hepatocytes from Abx-treated mice and

Cd1d^{-/-} mice (Fig. 6d); this difference might arise from the reduced number of endogenous lipid antigens presented by CD1d on Abx-treated hepatocytes. After supplying exogenous lipid antigens, WT or Abx-treated, but not *Cd1d*^{-/-}, hepatocytes induced an approximately twofold increase in the $\gamma\delta T-17$ cell number compared with those without exogenous lipid antigens added (Fig. 6e). These results indicate that hepatocytes can directly present commensal/*E. coli* lipid antigens through CD1d to promote liver-resident $\gamma\delta T-17$ cell expansion.

Hepatic $\gamma\delta T-17$ cell accelerate HFD-induced NAFLD progression.

Using an *Il17ra*^{-/-} mouse, Harley *et al.*²⁵ showed that IL-17A signalling could accelerate NAFLD through recruiting neutrophils and inducing nicotinamide adenine dinucleotide phosphate (NADPH) oxidase-dependent ROS, which ultimately induced hepatocellular damage. We wondered if the predominant liver-resident $\gamma\delta T-17$ cell subtype was the source of IL-17A during NAFLD, and, importantly, whether the microbiota promoted NAFLD through these cells.

High-fat diet (HFD)-fed mice displayed elevated numbers of $\gamma\delta T-17$ cells in several organs, including the liver (Fig. 7a, Supplementary Fig. 6a), suggesting that hepatic $\gamma\delta T-17$ cells might be one of the main sources of IL-17A in the liver during NAFLD. Though *Tcrd*^{-/-} mice a body weight increase comparable to that of WT mice (Supplementary Fig. 6b), they were protected from NAFLD by displaying reduced steatohepatitis, reduced liver damage and a catabolic glucose dysmetabolism (Fig. 7b–d). The reduced NAFLD symptoms in *Tcrd*^{-/-} mice were also displayed in another mouse NAFLD model induced by high-fat/high-carbohydrate diet (HFHCD) (Fig. 7e), and transfer

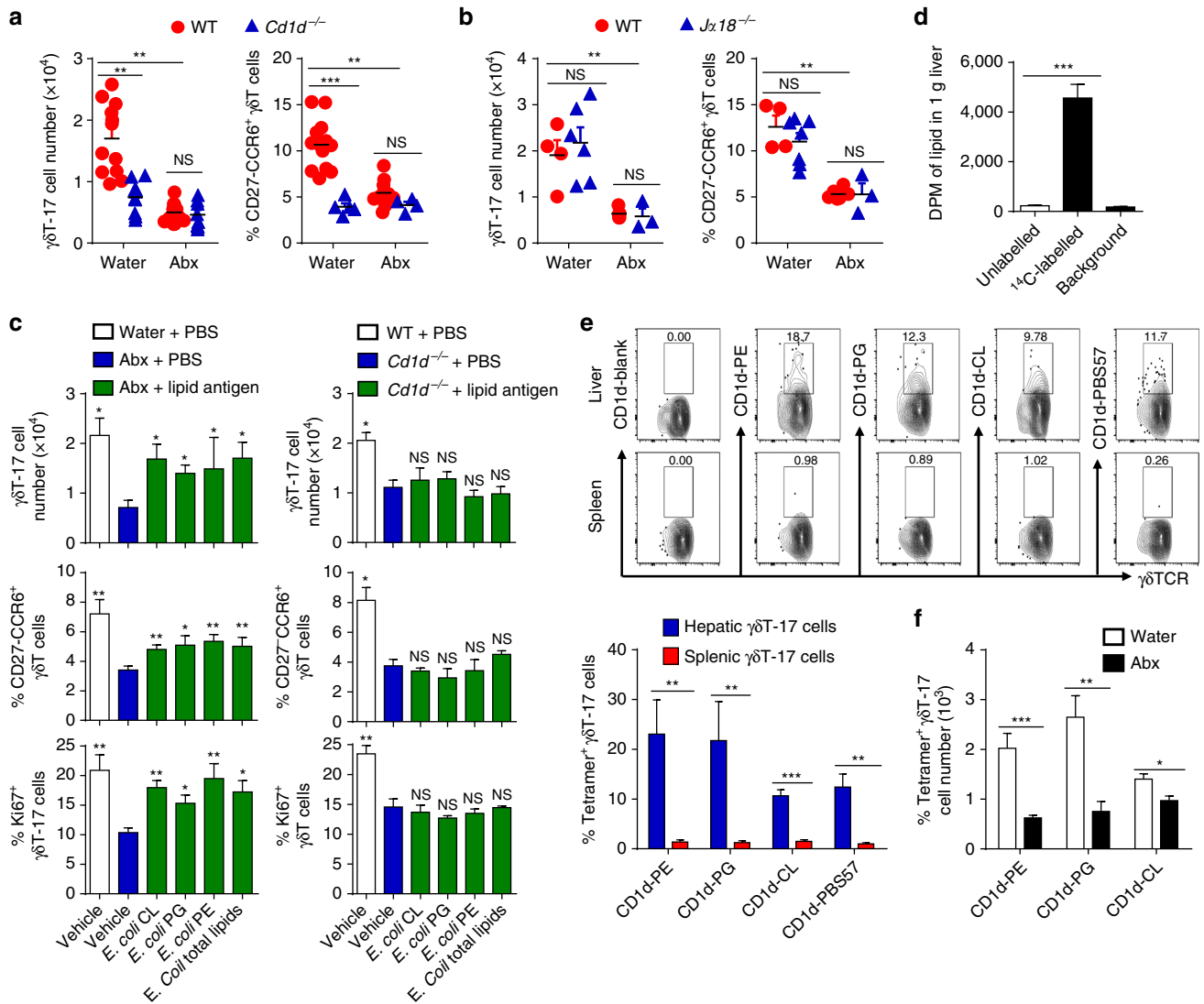


Figure 5 | *E. coli* lipid antigens promote hepatic $\gamma\delta$ T-17 cells in a CD1d-dependent manner. (a) Age-matched (3 weeks old) and co-housed WT and *Cd1d*^{-/-} mice were fed water alone (Water) or containing antibiotics (Abx) for 4 weeks, and IL-17A expression and phenotype markers of hepatic $\gamma\delta$ T cells were evaluated by FACS at 7 weeks old (each dot represents a mouse). (b) WT and *Jx18*^{-/-} mice were co-housed as in a, and the IL-17A expression and phenotype markers of hepatic $\gamma\delta$ T cells were then evaluated by FACS (each dot represents a mouse). (c) Abx-treated WT mice or normal water-treated *Cd1d*^{-/-} mice were i.p. injected with 20 μ g *E. coli* cardiolipin (CL), *E. coli* phosphatidylglycerol (PG), *E. coli* phosphatidylethanolamine (PE) or 50 μ g total *E. coli* polar lipid extract six times at 2-day intervals, and IL-17A expression, Ki67 expression and phenotype markers of hepatic $\gamma\delta$ T cells were evaluated by FACS (*n* = 5 per group). (d) Abx-treated mice were intragastrically administered 10¹⁰ c.f.u. of unlabelled or ¹⁴C-labelled *E. coli*, and the radioactivity of the lipids extracted from the liver was evaluated 6 h later (*n* = 3, 4, *n/a*; from left to right) (e) $\gamma\delta$ T-17 cells (gated CD45⁺ CD3⁺ TCR $\gamma\delta$ ⁺ IL-17A⁺) from the spleens and livers of WT mice were stained with CD1d tetramer loaded with the indicated lipid antigens, and the representative graph and cumulative data are shown (*n* = 4 per group). (f) Mice were treated with antibiotics, and the CD1d-lipid antigen tetramer-specific hepatic $\gamma\delta$ T-17 cell numbers were evaluated by FACS (*n* = 4 per group). The data are representative of three independent experiments and shown as the mean \pm s.e.m. (**P* < 0.05; ***P* < 0.01; ****P* < 0.001 one-way ANOVA with post hoc test).

of HFHCD-fed mice with WT hepatic $\gamma\delta$ T cells, but not with *Il17a*^{-/-} hepatic $\gamma\delta$ T cells, accelerated NAFLD in *Tcrd*^{-/-} mice (Fig. 7e). These results demonstrate that hepatic $\gamma\delta$ T-17 cells can accelerate NAFLD.

Next, we asked whether the microbiota were involved in hepatic $\gamma\delta$ T-cell expansion during NAFLD. Both HFD and HFHCD triggered the increase and proliferation of hepatic $\gamma\delta$ T-17 cells (Fig. 8a,b). However, after depleting commensal microbes, Abx-treated mice that started with lower hepatic $\gamma\delta$ T-cell numbers had only slight increases compared with the baseline of control mice, and the numbers was far lower than the levels observed in HFD/HFHCD-induced NAFLD mice

(Fig. 8a,b). Another candidate for microbiota associated-IL-17A production was Th-17 cells; unlike Th-17 cells in the intestine²⁶ and skin²⁷, which can be induced to proliferation by their local microbiota, the numbers of hepatic Th-17 cells did not decrease in Abx-treated mice, and HFD and HFHCD did not trigger increased hepatic Th-17 cells, indicating the irrelevant role of hepatic Th-17 cells in this process (Fig. 8c). The downstream effectors of IL-17A during NAFLD²⁵, the numbers of neutrophils (Fig. 8d), and the mRNA levels of NADPH oxidase enzymes (Fig. 8e) also decreased in the livers of Abx-treated mice.

More importantly, Abx-treated mice exhibited a similar alleviation of NAFLD as *Tcrd*^{-/-} mice fed with HFD/HFHCD,

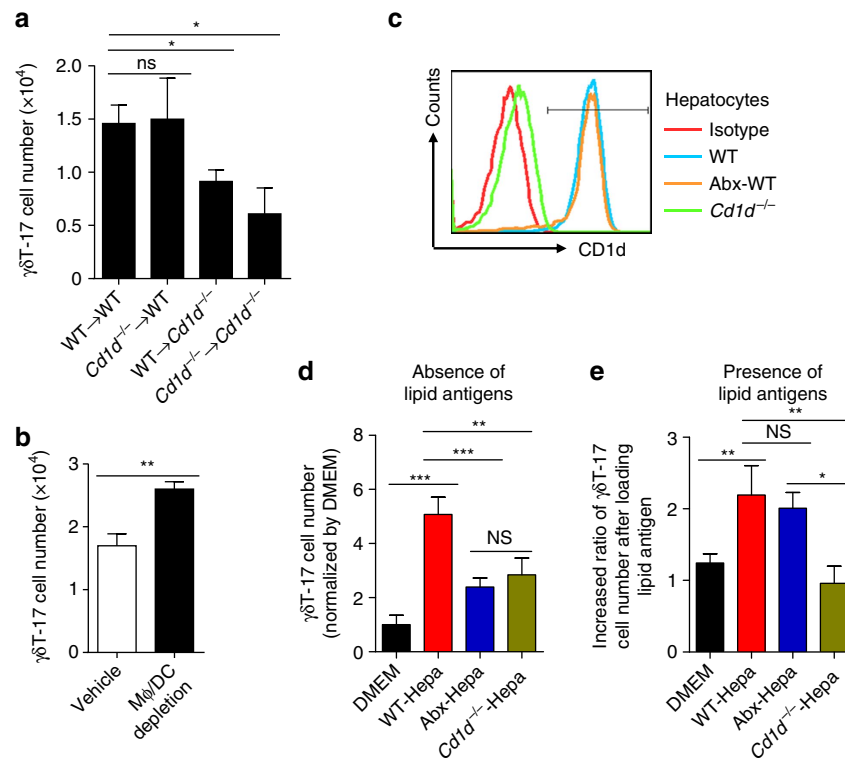


Figure 6 | Hepatocytes loaded with lipid antigen promote hepatic $\gamma\delta$ T-17 cells *in vitro*. (a) Quantification of hepatic $\gamma\delta$ T-17 cells from chimeric mice reconstructed with fetal liver MNCs ($n=4$ per group). (b) The numbers of hepatic $\gamma\delta$ T-17 cells from vehicle- or clodronate liposome-treated WT mice ($n=4, 5$). (c) CD1d expression on the indicated hepatocytes. (d) Purified hepatic $\gamma\delta$ T cells from WT mice were co-cultured with the indicated hepatocytes for 3 days, and the $\gamma\delta$ T-17 cell number (normalized by the DMEM group) was analysed by FACS ($n=6$ wells per group). (e) Purified $\gamma\delta$ T cells were co-cultured with lipid antigen-loaded hepatocytes for 3 days. The increased ratios of $\gamma\delta$ T-17 cell numbers compared with those without added lipid antigens are shown ($n=6$ wells per group). The data are representative of three independent experiments and shown by the mean \pm s.e.m. (* $P<0.05$; ** $P<0.01$; *** $P<0.001$ unpaired Student's *t*-test (b), one-way ANOVA with post hoc test (a,d,e).

as indicated by the reduced steatohepatitis (Fig. 9a,b), the reduced ALT level (Fig. 9c), the elevated body weight (Fig. 9d) and the catabolic glucose dysmetabolism (Fig. 9e). The reduced liver damage, elevated hepatic triglyceride level, elevated body weight and catabolic glucose dysmetabolism in Abx-treated mice could be reversed by transferring $\gamma\delta$ T cells or IL-17A protein (Fig. 9f–i). Together, these data suggest that the microbiota function as a co-factor to accelerate HFD/HFCD-triggered NAFLD *via* increasing hepatic $\gamma\delta$ T-17 cells.

Discussion

To our knowledge, our study is the first to describe the unique characteristics and mechanisms of liver-resident $\gamma\delta$ T cells controlled by the microbiota. First, they are liver resident without exchanging with circulating $\gamma\delta$ T cells (Fig. 1e and Supplementary Fig. 1a–c); second, hepatic $\gamma\delta$ T cells predominantly produce a high level of IL-17A (Fig. 1a–d); third, they specifically recognize (Fig. 5e) and are promoted by (Figs 5c and 6d,e) CD1d/commensal lipid antigen.

$\gamma\delta$ T-17 cells originate from fetal $\gamma\delta$ thymocytes and are preferentially located in barrier tissues²⁸. The heterogeneity of $\gamma\delta$ T cells in different locals is more common than previously thought. Skin $\gamma\delta$ T-17 cells are compartmentally controlled by the skin, but not gut, microbiota²⁷; IL-1R signalling has an important role in microbiota-mediated IL-17A production by PC $\gamma\delta$ T cells²¹; IL-17A production by lung-resident $\gamma\delta$ T cells requires IL-6 signalling instead²⁹; dermal $\gamma\delta$ T cells preferentially rely on IL-1 and MyD88 signalling to produce IL-17A³⁰; the $\gamma\delta$ T-cell subtype in the colonic lamina propria produces

IL-17A in an IL-23-independent manner³¹. Thus these findings together with the mechanism of liver $\gamma\delta$ T-cell homeostasis found by us, further indicate that the host–microbiota interaction at distinct barrier sites occurs in a tissue-specific manner³².

IL-17A production by $\gamma\delta$ T cells is often elicited by cytokines or TLRs without prior antigen exposure (termed ‘natural $\gamma\delta$ T-17’ cells)³³, and we showed that TLR and IL-1/IL-23 signalling was not responsible for liver $\gamma\delta$ T-17 cell homeostasis in a physiological state (Supplementary Fig. 5). These two seemingly contradictory facts together exposed the mystery between $\gamma\delta$ T-cell antigen recognition and TLR/cytokine recognition. Increasing numbers of studies have indicated that encountering antigen is a prerequisite for $\gamma\delta$ T cells to respond to inflammatory cytokines^{34,35}. Until now, the antigen specificity or antigen requirement of the ‘natural $\gamma\delta$ T-17’ cells has remained unknown or controversial^{10,28}. However, although $\gamma\delta$ T cells in the mucosa and epithelium are well-suited to recognize microbial components, their recognized antigens remain scarce²⁸. In our study, we demonstrate for the first time that commensal lipid antigens can reach the liver (Fig. 5d) and be presented by CD1d to the $\gamma\delta$ TCR of liver-resident $\gamma\delta$ T cells (also a type of ‘natural $\gamma\delta$ T-17’) (Figs 5e and 6d,e), which supports the development and homeostasis of this cell subset.

The lipid antigens that specifically link CD1d and the $\gamma\delta$ TCR include bacterial CL³⁶, synthetic α -GalCer³⁷, sulfatide^{11,38}, synthetic phosphatidylcholine, PE, PG¹² and synthetic and natural PE³⁹. Among these, CL, PG and PE can be derived from both bacteria and stressed host cells^{40,41}. Indeed, *E. coli* CL,

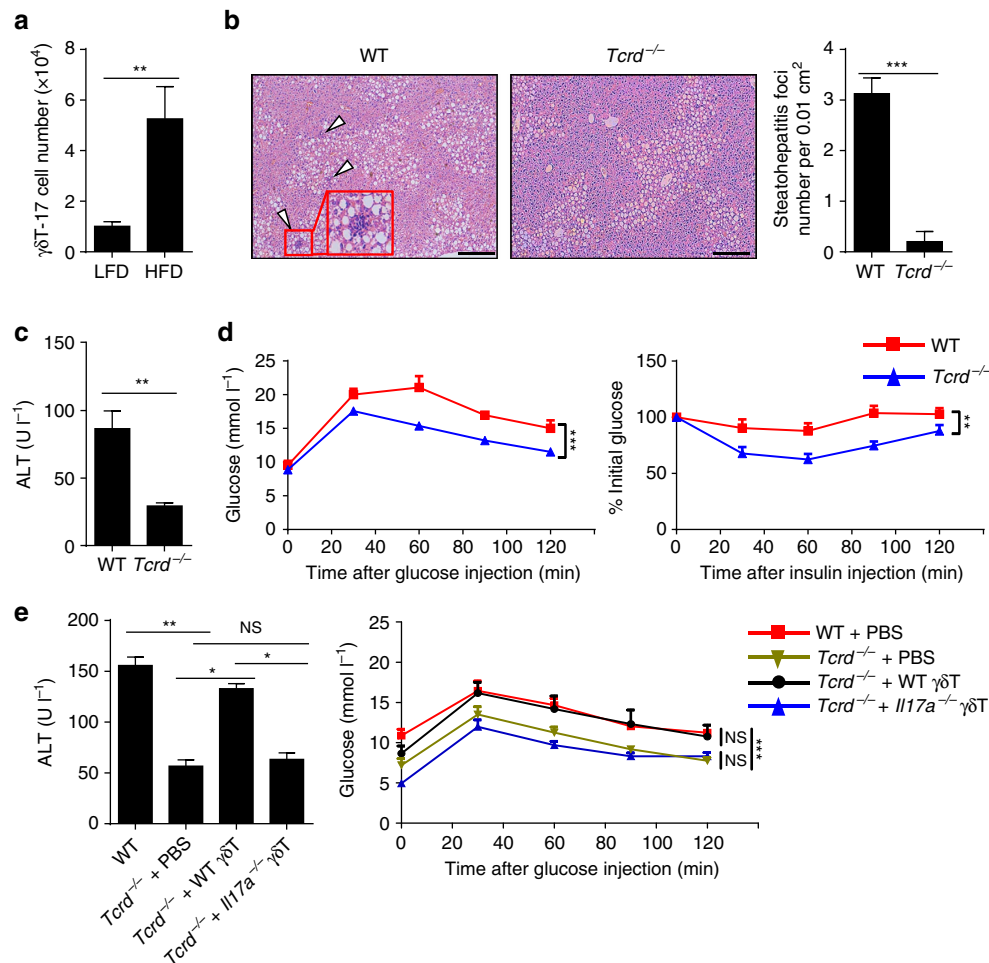


Figure 7 | Hepatic $\gamma\delta$ T-17 cells are essential for inducing NAFLD. (a) WT mice were placed on an HFD for 24 weeks, and the hepatic $\gamma\delta$ T-17 cell number was detected by FACS ($n = 4, 5$). (b–d) WT mice and $Tcrd^{-/-}$ mice were placed on an HFD for 24 weeks. (b) Representative liver histology (H&E staining, scale bar, 200 μ m); arrowheads indicate the steatohepatitis foci of inflammation with clusters of inflammatory cells, and the red rectangle indicates a 4 \times zoom of the gated region ($n = 4, 5$). (c) The serum ALT level ($n = 4, 5$), (d) glucose tolerance test (GTT) curve and insulin tolerance test (ITT) curve were assessed ($n = 4, 9$). (e) HFHCD-fed $Tcrd^{-/-}$ mice were either i.v. transferred with WT hepatic $\gamma\delta$ T cells or $Il17a^{-/-}$ hepatic $\gamma\delta$ T cells (2×10^4 , once per week) from the 4th week to the 10th week during HFHCD treatment, and the serum ALT level and GTT curve were evaluated ($n = 4$ per group). The data are representative of three independent experiments and shown by the mean \pm s.e.m. (* $P < 0.05$; ** $P < 0.01$; *** $P < 0.001$ unpaired Student's t -test (a, b, c), one-way ANOVA post hoc test (e, left panel), two-way ANOVA test (d, e right panel).

PG and PE could partly recover the decreased hepatic $\gamma\delta$ T-17 cells in Abx-treated mice (Fig. 5c); nevertheless, none of these antigens could completely recover the decline, suggesting that other lipid antigens may also have roles in this process. We showed that liver $\gamma\delta$ T-17 cells could also be stained by CD1d-PBS57 tetramer (an improved form of α -GalCer²³) (Fig. 5e), which may be a result of the cross-reactivity of the CD1d-lipid antigens recognized by the $\gamma\delta$ TCR. The cross-reactivity of CD1d-phospholipids and CD1d- α -GalCer³⁷, as well as that of CD1d-CL and CD1d-phospholipids⁴², were also observed in other $\gamma\delta$ TCR studies.

Several types of hepatic cells, including endothelial cells, Kupffer cells and DCs, can express CD1d, but the strongest CD1d-expressing cell is hepatocytes, which are also critical lipid metabolic factories²⁴. Furthermore, CD1d expression on hepatocytes is the main component of hepatic T-cell-lipid antigen recognition¹³. Investigators previously observed that CD1d on hepatocytes could activate NKT cells^{14–16}. Our study demonstrated that hepatocytes can also promote $\gamma\delta$ T-17 cells in the presence of lipid antigens (Fig. 6c–e). The difference in lipid antigen recognition by the TCR of $\gamma\delta$ T cells and that of NKT cells

is an interesting topic. For example, although CD1d can present α -GalCer to both $\gamma\delta$ T cells and NKT cells, the mode of $\gamma\delta$ TCR-CD1d- α -GalCer recognition appears to be markedly different from that of NKT recognition³⁷. Thus, the difference between NKT and $\gamma\delta$ T cells in CD1d recognition of microbiota-derived lipid antigens requires further investigation.

NAFLD is induced by chronic inflammation in obesity, and the progression of NAFLD is the comprehensive result of hepatic immune cells, including Kupffer cells⁴³, NK cells⁴⁴ and NKT cells⁴⁵, and liver metabolic cells, including hepatocytes and hepatic stellate cells^{44,46}. However, although the metabolic relationship between the microbiota and fatty liver has been shown, how the microbiota influences the hepatic immune response during NAFLD remains unclear^{47–49}. In this study, we showed that microbiota-maintained liver-resident $\gamma\delta$ T-17 cells were the main source of IL-17A and could significantly accelerate NAFLD (Fig. 7). An interesting finding was the uncoupling of decreased liver inflammation (Fig. 9a–c) and increased body weight (Fig. 9d) in Abx-treated mice, which was also found by other groups in $Il17ra^{-/-}$ mice²⁵ and Abx-treated mice⁵⁰. However, this uncoupling was not found in $Tcrd^{-/-}$ mice, who

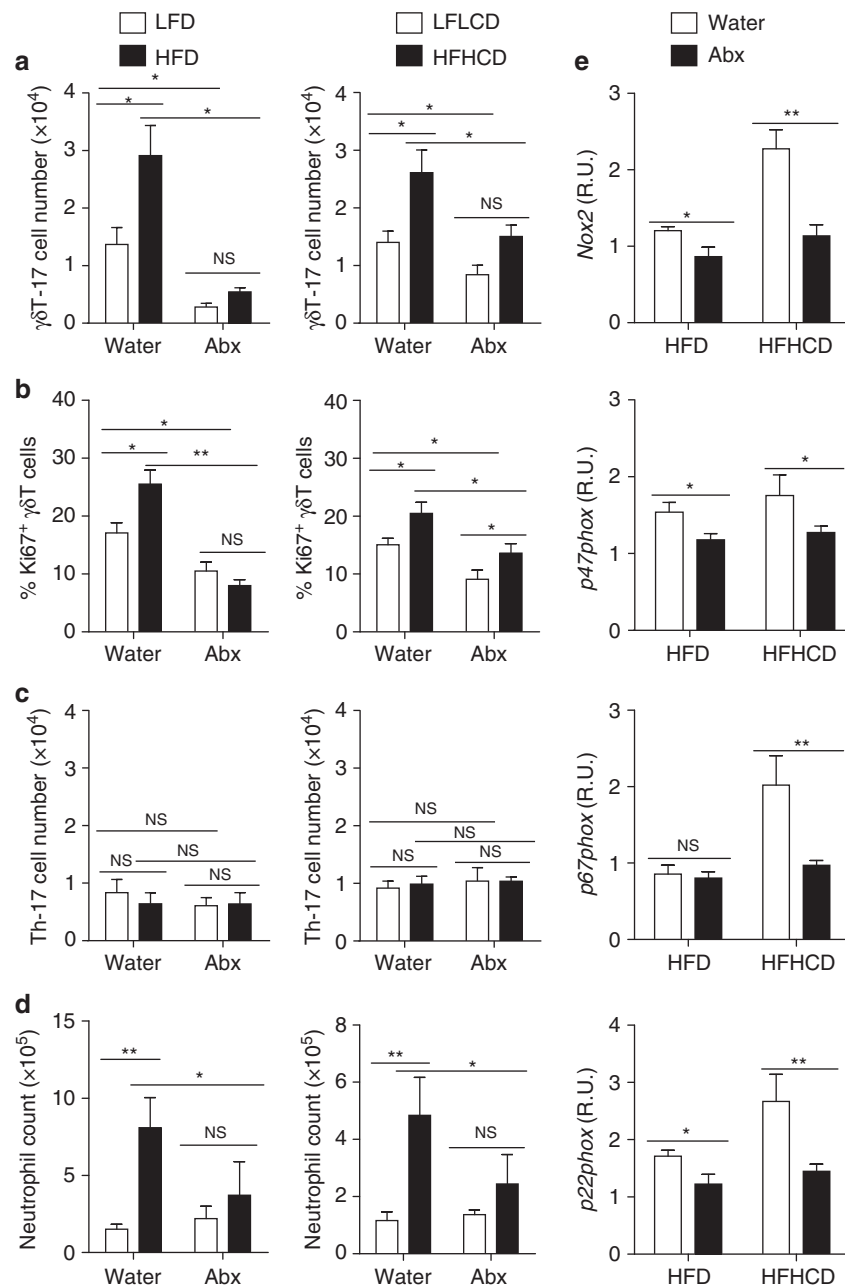


Figure 8 | The microbiota promote the expansion of liver-resident $\gamma\delta$ T-17 cells during HFD/HFHCD-induced NAFLD. Normal water-fed mice and Abx-treated B6 mice were placed on an HFD (LFD as control) and an HFHCD (LFLCD as control) for 24 weeks. **(a)** The hepatic $\gamma\delta$ T-17 cell number, **(b)** Ki67 expression of hepatic $\gamma\delta$ T cells, **(c)** hepatic Th-17 cell number and **(d)** neutrophil number in the liver were detected by FACS. **(e)** Water- and Abx-treated B6 mice were placed on an HFD or an HFHCD for 12 weeks. The hepatic mRNA expression levels of *Nox2*, *p47phox*, *p67phox* and *p22phox* were evaluated. The data are representative of three independent experiments with five mice per group and shown by the mean \pm s.e.m. (* $P < 0.05$; ** $P < 0.01$; *** $P < 0.001$ one-way ANOVA with post hoc test.).

displayed reduced liver inflammation (Fig. 7b–e) but comparable body weights to those of WT mice, as shown by us (Supplementary Fig. 6b) and others⁵¹. This suggests that different mechanisms are used by IL-17A to promote hepatic inflammation and lipid metabolism and that the lipid metabolism pathway might be compensated for by other signals in *Tcrd*^{-/-} mice.

After depleting commensal microbes, hepatic $\gamma\delta$ T-17 cells did not increase (Fig. 8a), but they did increase in the presence of microbiota during NAFLD. Nevertheless, same as $\gamma\delta$ T-17 cells in the liver, $\gamma\delta$ T-17 cells in the gut and other tissues also increase during NAFLD (Supplementary Fig. 6a), mainly because NAFLD

is a systemic disease with inflammation in multiple organs⁵². Thus, though there is no mutual exchange or circulation between hepatic $\gamma\delta$ T cells (Fig. 1e) and gut $\gamma\delta$ T cells⁵³ at steady state, we still cannot fully exclude the possibility that a portion of gut $\gamma\delta$ T-17 cell would traffic to the liver in the disease state. However, instead of the cellular traffic model, we depict a molecular traffic model by displaying that *E. coli* lipid can reach the liver from gut (Fig. 5d); then the lipid antigen can be presented by hepatocyte-expressed CD1d to directly stimulate hepatic $\gamma\delta$ T cells (Fig. 6c–e) and ultimately alleviate hepatic $\gamma\delta$ T-17 cell clones that are specific to CD1d-lipid antigen tetramer (Fig. 5e). Nevertheless, four possible mechanisms exist for the accumulation of hepatic $\gamma\delta$ T-17 cell

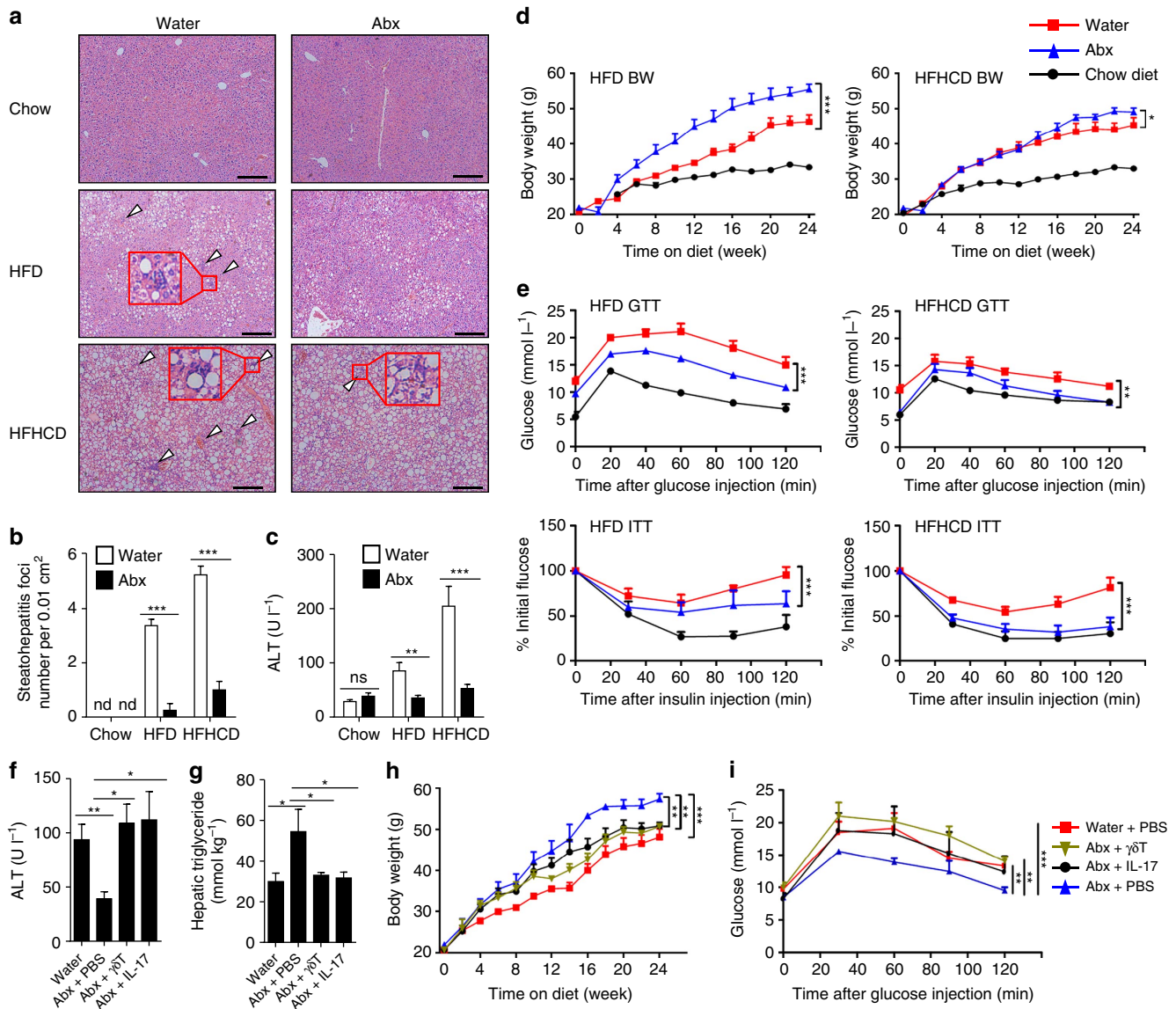


Figure 9 | The microbiota accelerate HFD/HFHCD-induced NAFLD through hepatic $\gamma\delta$ T-17 cells. (a–e) Mice were treated as described in Fig. 8. (a) Representative liver histology (H&E staining, scale bar, 200 μ m); arrowheads indicate the steatohepatitis foci of inflammation with clusters of inflammatory cells, and the red rectangle indicates a 4 \times zoom of the gated region. (b) Numbers of steatohepatitis foci counted in a ($n=5$ per group). (c) Serum ALT level, (d) body weight curve and (e) glucose tolerance test (GTT) and insulin tolerance test (ITT) curves are shown ($n=5$ per group). (f–i) HFD-fed, Abx-treated mice were either injected with IL-17A (500 ng, once per week) or transferred with hepatic $\gamma\delta$ T cells (2×10^4 , once per 2 weeks) from the 4th week to the 24th week of HFD treatment, (f) The serum ALT level, (g) hepatic triglyceride level, (h) body weight curve and (i) GTT curve are shown ($n=5$ per group). The data are representative of three independent experiments and shown by the mean \pm s.e.m. (* $P < 0.05$; ** $P < 0.01$; *** $P < 0.001$ one-way ANOVA with post hoc test (b,c,f,g), two-way ANOVA test (d,e,h,i).

during NAFLD from our analysis. First, the excessive accumulation of fat-related lipid antigens during NAFLD may further affect hepatic $\gamma\delta$ T-17 cells; because it is difficult to distinguish the sources of lipids *in vivo*, there is still more work to do. Second, because NAFLD is always accompanied by the over growth of commensal microbes^{47–49}, an elevated global microbe load or several specific bacteria may induce a higher number of hepatic $\gamma\delta$ T-17 cells as described in our study. Third, HFD-induced inflammation may stimulate the microbiota-maintained hepatic $\gamma\delta$ T-17 cells as a bystander effect. Forth, there may be a portion of $\gamma\delta$ T-17 cells activated in other tissues (for example, gut) traffic into the liver.

Similar to that observed in the mouse liver, healthy human livers also contain a distinct V δ 3⁺ $\gamma\delta$ T-cell subset⁵⁴; interestingly, they recognize CD1d and release IL-17A after

activation⁵⁵. However, their detailed characteristics and precise mechanisms are unclear. Using a mouse model, our work demonstrates for the first time that hepatic $\gamma\delta$ T cells are a unique liver-resident subset. Hepatocyte CD1d could present gut commensal lipid antigens to hepatic $\gamma\delta$ T cells, which drove them to predominantly produce IL-17A and maintained their haemostasis. Our results reveal a novel crosstalk between metabolism and immunity in the liver–gut axis and also suggest a tissue-specific interaction between the microbiota and immune cells in the liver (Supplementary Fig. 7).

Methods

Mice. C57BL/6 mice were purchased from the Shanghai Laboratory Animal Center (SLAC, Chinese Academy of Sciences); *Rag1*^{-/-} mice were obtained from the Model Animal Research Center (Nanjing University); *Cxcr6*^{sfp/gfp} and CD45.1⁺

mice were purchased from the Jackson Laboratory; *Tcrd*^{-/-} mice were a gift from Dr Zhinan Yin (Nankai University); *Tlr2*^{-/-}, *Tlr4*^{-/-} and *Tlr9*^{-/-} mice were a gift from Dr Shaobo Su (Sun Yat-sen University); *Il17a*^{-/-} mice were a gift from Dr Zhexiong Lian (University of Science and Technology of China (USTC)); and *Jα18*^{-/-} and *Cd1d*^{-/-} mice were a gift from Dr Li Bai (USTC). All of the above mice were housed in a specific pathogen-free facility and all of the animal protocols were approved by Local Ethics Committee for Animal Care and Use at University of Science and Technology of China. Germ-free mice were purchased from SLAC and housed in the germ-free facility at SLAC according to their animal care regulations. The sample size was determined by the 'resource equation' method, taking into account the possible reduction of diet/drink treatment.

Mouse treatment. Six- to ten-week-old male mice were used in most of the experiments with exceptions, such as the use of neonatal mice in the ontogeny experiment and the use of 30-week-old mice in the HFD/HFCD-induced NAFLD experiment. Commensal microbes were depleted using antibiotics as previously reported²⁰, the detailed method are followed. Four kinds of antibiotics including ampicillin (1 g l⁻¹), vancomycin (0.5 g l⁻¹), neomycin sulfate (1 g l⁻¹) and metronidazole (1 g l⁻¹) were dissolved in sterile water and stored in 4 °C no more than a week before using. This antibiotic-containing water was supplied as drinking water to adult mice and pregnant mice for more than 4 weeks and was changed every 3 days. The volume of drinking water and the body weights of the mice were monitored twice a week. Mice exhibiting more than a 30% decline in body weight were removed. After antibiotic treatment stopped, Abx-treated mice were co-housed with normal mice for 4 weeks to reconstitute commensals.

For the PAMP restoration experiment, WT mice and Abx-treated mice were intraperitoneally (i.p.) injected with 50 µg curdlan, 50 µg Pam3csk4, 100 µg LPS, 100 µg poly(I:C) or 50 µg CpG (all from Sigma) and harvested 1 day later. For cytokine neutralization, the mice were intravenously (i.v.) injected with 50 µg control IgG, anti-IL-1β or anti-IL-23 antibody twice at 3-day intervals and harvested 3 days later. For the lipid antigen restoration experiment, the mice were i.p. injected with 20 µg *E. coli* CL, PG or PE or 50 µg *E. coli* polar lipid extract (all from Avanti Polar Lipids, Alabama) six times at 2-day intervals and harvested 2 days after the last injection. For macrophage and DC depletion, the mice were i.v. injected with 200 µl C12MDP-Lip (Vrije Universiteit) twice at 3-day intervals and harvested 3 days later. All of the mice receiving the above treatment were randomly assigned to different groups, but the investigators were not blinded to the treatments or genotypes.

Bacterial diversity analysis. Fresh stool samples were collected and weighed, and bacterial DNA was extracted from the stool using a QIAamp Fast DNA Stool Mini Kit (Qiagen). The 16S rRNA gene was analysed to determine the bacterial composition and diversity using an Illumina MiSeq (Novogene Bioinformatics Technology Co., Ltd).

For bacterial titre analysis, fresh stools were collected and homogenized in sterile PBS. The serially diluted homogenates were plated onto blood agar plates (for total cultivable bacterial determination) or eosin methylene blue (EMB; for *E. coli* determination) plates at 37 °C for 24 h. The colonies were distinguished by their biochemical reactions and counted.

Faeces/*E. coli* transfer. Mice were treated with antibiotics for 4 weeks, and their antibiotic-containing water was replaced with antibiotic-free water. Then, the mice were intragastrically administered 0.2 ml fresh faeces (50 mg ml⁻¹) or 10⁸/10⁹/10¹⁰ c.f.u. of *E. coli* that was isolated from an EMB plate and expanded in LB. The mice were analysed 3 weeks later.

¹⁴C labelling of *E. coli*. *E. coli* was ¹⁴C labelled as previously reported⁵⁶ with a slight modification. Briefly, *E. coli* was isolated from fresh mouse faeces using an EMB plate, expanded in M9 minimal medium to OD₆₀₀ = 0.4 and spiked with 25 µCi/L ¹⁴C-glucose (NEC042V250UC, PerkinElmer) for 16 h. A total of 10¹⁰ c.f.u. of unlabelled or ¹⁴C-labelled *E. coli* was intragastrically delivered to the mice. The livers were collected 6 h later, the lipids in the liver were extracted using a methanol/chloroform (2:1) mixture and radioactivity was assessed.

Parabiosis. CD45.1⁺ and CD45.2⁺ mice were joined by parabiosis for 2 weeks as previously described⁵⁷. Age matched and co-housed mice were anaesthetic and shaved. An incision along the lateral aspect of each mouse was made. The mice were then sutured together at the elbow and knee as well as at the skin around the incision. Mice were i.p. injected with 5% glucose and 0.9% sodium chloride to recover energy and water. Buprenex was used to relieve pain. Sulfatrim was added to the drinking water for 7 days.

NAFLD model. Mice were placed on two model diets and matched control diets. HFD (60% of kcal fat, carbohydrate 20% kcal, protein 20% kcal; Research Diets #D12492) and LFD (10% of kcal fat, carbohydrate 70% kcal, protein 20% kcal; Research Diets #D12450B) and the corresponding HFCD (fat 42% kcal, carbohydrate 42.7% kcal, protein 15.3% kcal; TROPIC Animal Feed High-Tech Co.

#TP26301⁺ carbohydrates (18.9 g l⁻¹ sucrose + 23.1 g l⁻¹ fructose) in drinking water) and LFLCD (fat 12.5% kcal, carbohydrate 68.1% kcal, protein 19.4% kcal; TROPIC Animal Feed High-Tech Co. #TP26323 + carbohydrate-free drinking water). Fresh food was supplied twice a week, and the food and drink consumption were quantified throughout the experiment. The body weights of the mice were monitored weekly.

For the IL-17A and hepatic γδT-cell transfer experiment, Abx-treated mice were i.v. injected with IL-17A protein (PeproTech, 500 ng, once per week) or purified hepatic γδT cells (2 × 10⁴, once per 2 weeks) from the 4th week on an HFD until harvesting at the 24th week. *Tcrd*^{-/-} mice were i.v. injected with purified hepatic γδT cells (2 × 10⁴, once per week) from the 4th week on a HFCD until collecting at the 10th week.

For the GTT test, mice were fasted for 12 h and i.p. injected with 1 g kg⁻¹ glucose; for the ITT test, mice were fasted for 3 h and i.p. injected with 0.5 U kg⁻¹ human fast-acting insulin (Lilly France). Tail vein blood was collected both pre-injection and at various times post injection of glucose or insulin. The glucose levels in the blood were assayed by an automated glucometer (LifeScan). Serum ALT and AST were determined using an automated Chemray 240 clinical analyzer (Rayto, Shenzhen, China). Liver samples that were fixed in 4% paraformaldehyde and paraffin-embedded were sliced into 5-µm-thick sections and stained with H&E. Lipids in the frozen liver tissue were extracted using a methanol/chloroform (2:1) mixture and dissolved in isopropyl alcohol. The triglyceride level was detected using a kit (Huili, China).

Cell preparation. Mice were killed, and the iLNs, spleens, livers, lungs, thymi, intestines, colons and mesenteric LNs were collected. Mononuclear cells (MNCs) from each organ were then separated as previously described with slight changes⁵⁸. Briefly, LNs and thymi were passed through a 200-gauge steel mesh and washed with PBS. Spleens were first passed a 200-gauge steel mesh then RBC lysed and washed with PBS. Livers were passed a 200-gauge steel mesh and the cell pellet were collected in the flow through, the MNCs in the pellets were isolated by gradient centrifugation with 40 and 70% Percoll. Lungs were first excised and minced to small pieces, then digested with 0.1% collagenase I for 1 h at 37 °C, the large pieces of lung were removed by filtering and the MNCs in the flow through were obtained by gradient centrifugation with 40 and 70% Percoll. Intestines and colons were surgically exclude the peyer's patch and then excised to small pieces, digested with 1 mM DTT for 15 min at 37 °C and passed a 200-gauge mesh, IEL in the flow through were isolated by gradient centrifugation with 40 and 70% Percoll, the unfiltered tissue was further digested with collagenase IV for 1 h at 37 °C and filtered with 200-gauge mesh, LPL in the flow through were isolated by gradient centrifugation with 40 and 70% Percoll. PC MNCs were obtained by peritoneal lavage using cold PBS. Hepatic γδT cells were purified using a mouse TCRγδ⁺ T-Cell Isolation Kit (Miltenyi Biotec).

Fetal liver MNC chimera. To construct a hematopoietic chimera, 2 × 10⁶ fetal liver MNCs from an E18.5 mouse were transferred to lethally irradiated 10-week-old mice (11 Gy, 1 day before transfer). Hepatic γδT cells were analysed 20 weeks later.

In vitro co-culture. Hepatocytes were separated using a previously described two-step perfusion method⁵⁹. Briefly, mice were anaesthetized and the portal vein was cannulated. The liver was first digested with 0.5 mM EGTA and then digested with 0.05% collagenase IV, the digested liver resuspension was passed a 200-gauge steel mesh and the hepatocytes in the flow through were isolated by 40% Percoll. Hepatocytes (5 × 10⁴ per well) were pre-cultured for 24 h to adhere, during which mixed lipid antigens (2.5 µg ml⁻¹ PG, PE and CL, dissolved in ethanol and chloroform) were loaded or not loaded onto the cells. Then, the hepatocytes were washed and co-cultured with purified hepatic γδT cells (1 × 10⁴ per well) for 3 days. IL-17A expression was detected by FACS, and the cell number was counted.

Flow cytometry analysis. Freshly isolated MNCs were blocked and incubated with the indicated fluorescent mAbs for 30 min at 4 °C. The cells were stimulated with 50 ng ml⁻¹ PMA (Sigma) and 1 µg ml⁻¹ ionomycin (Sigma) and treated with 10 µg ml⁻¹ monensin (Sigma), and the cells were then blocked with rat serum and stained for surface markers, fixed, permeabilized and labelled with the indicated intracellular antibody. Antibody information is summarized in Supplementary Table 1. All samples were collected on an LSRII flow cytometer (BD Biosciences) and analysed using FlowJo software (Tree Star). The gating strategy is showed in Supplementary Fig. 8.

CD1d-lipid antigen tetramer. Brilliant Violet 421-labelled PBS-57-loaded and unloaded mCD1d tetramers were kindly provided by the NIH tetramer core. Unloaded mCD1d tetramer (1 mg ml⁻¹, 100 µl) was conjugated with lipid antigens (1 mg ml⁻¹ PE, PG or CL, 20 µl) in PBS buffer containing 1 µM pepstatin, 1 µg ml⁻¹ leupeptin and 2 mM EDTA, which was then washed and concentrated using a 30 K microconcentrator (Amicon Ultra-15, Millipore UFC903024). The cells were stained with other antibodies as described in the flow cytometry analysis section, collected on a SP6800 spectral analyzer (Sony Biotechnology Inc.), and

analysed using FlowJo software with a gating strategy showed in Supplementary Fig. 8.

BrdU incorporation. Mice were i.p. injected with 1 mg BrdU three times at 2-day intervals. The BrdU⁺ cell frequency was evaluated according to the FITC BrdU Flow Kit instructions (BD Pharmingen).

Quantitative RT-PCR. Total RNA from liver tissue was extracted using TRIzol reagent (Invitrogen). Gene expression was analysed according to the instructions of the SYBR Premix Ex Taq kit (Takara) and quantified using the $\Delta\Delta C_t$ method. All primers (Supplementary Table 2) were synthesized by Sangon (Shanghai, China).

Statistics. Student's *t*-test for two groups and a one-way ANOVA for more than two groups were used to determine statistically significant differences. A two-way ANOVA test was used to determine differences in the GTT and ITT tests. Differences achieving values of $P < 0.05$ were considered statistically significant.

Data availability. The data that support the findings of this study are available within the article and its Supplementary Information files or from the corresponding authors on request.

References

- Racaneli, V. & Rehermann, B. The liver as an immunological organ. *Hepatology* **43**, S54–S62 (2006).
- Gao, B., Jeong, W. I. & Tian, Z. Liver: An organ with predominant innate immunity. *Hepatology* **47**, 729–736 (2008).
- Jenne, C. N. & Kubes, P. Immune surveillance by the liver. *Nat. Immunol.* **14**, 996–1006 (2013).
- Henao-Mejia, J., Elinav, E., Thaiss, C. A., Licona-Limon, P. & Flavell, R. A. Role of the intestinal microbiome in liver disease. *J. Autoimmun.* **46**, 66–73 (2013).
- Chassaing, B., Etienne-Mesmin, L. & Gewirtz, A. T. Microbiota-liver axis in hepatic disease. *Hepatology* **59**, 328–339 (2014).
- Bonneville, M., O'Brien, R. L. & Born, W. K. Gammadelta T cell effector functions: a blend of innate programming and acquired plasticity. *Nat. Rev. Immunol.* **10**, 467–478 (2010).
- Hayday, A. C. Gammadelta T cells and the lymphoid stress-surveillance response. *Immunity* **31**, 184–196 (2009).
- Hammerich, L. & Tacke, F. Role of gamma-delta T cells in liver inflammation and fibrosis. *World J. Gastrointest. Pathophysiol.* **5**, 107–113 (2014).
- Salio, M., Silk, J. D., Jones, E. Y. & Cerundolo, V. Biology of CD1- and MR1-restricted T cells. *Annu. Rev. Immunol.* **32**, 323–366 (2014).
- Luoma, A. M., Castro, C. D. & Adams, E. J. gammadelta T cell surveillance via CD1 molecules. *Trends Immunol.* **35**, 613–621 (2014).
- Bai, L. *et al.* The majority of CD1d-sulfatide-specific T cells in human blood use a semiinvariant Vdelta1 TCR. *Eur. J. Immunol.* **42**, 2505–2510 (2012).
- Russano, A. M. *et al.* CD1-restricted recognition of exogenous and self-lipid antigens by duodenal gammadelta + T lymphocytes. *J. Immunol.* **178**, 3620–3626 (2007).
- Agrati, C. *et al.* CD1d expression by hepatocytes is a main restriction element for intrahepatic T-cell recognition. *J. Biol. Regul. Homeost. Agents* **19**, 41–48 (2005).
- Yang, L., Jhaveri, R., Huang, J., Qi, Y. & Diehl, A. M. Endoplasmic reticulum stress, hepatocyte CD1d and NKT cell abnormalities in murine fatty livers. *Lab. Invest.* **87**, 927–937 (2007).
- Zeissig, S. *et al.* Hepatitis B virus-induced lipid alterations contribute to natural killer T cell-dependent protective immunity. *Nat. Med.* **18**, 1060–1068 (2012).
- Yanagisawa, K. *et al.* Ex vivo analysis of resident hepatic pro-inflammatory CD1d-reactive T cells and hepatocyte surface CD1d expression in hepatitis C. *J. Viral. Hepat.* **20**, 556–565 (2013).
- Ribot, J. C. *et al.* CD27 is a thymic determinant of the balance between interferon-gamma- and interleukin 17-producing gammadelta T cell subsets. *Nat. Immunol.* **10**, 427–436 (2009).
- Paust, S. *et al.* Critical role for the chemokine receptor CXCR6 in NK cell-mediated antigen-specific memory of haptens and viruses. *Nat. Immunol.* **11**, 1127–1135 (2010).
- Wehr, A. *et al.* Chemokine receptor CXCR6-dependent hepatic NK T Cell accumulation promotes inflammation and liver fibrosis. *J. Immunol.* **190**, 5226–5236 (2013).
- Rakoff-Nahoum, S., Paglino, J., Eslami-Varzaneh, F., Edberg, S. & Medzhitov, R. Recognition of commensal microflora by toll-like receptors is required for intestinal homeostasis. *Cell* **118**, 229–241 (2004).
- Duan, J., Chung, H., Troy, E. & Kasper, D. L. Microbial colonization drives expansion of IL-1 receptor 1-expressing and IL-17-producing gamma/delta T cells. *Cell Host Microbe* **7**, 140–150 (2010).
- Balmer, M. L. *et al.* The liver may act as a firewall mediating mutualism between the host and its gut commensal microbiota. *Sci. Transl. Med.* **6**, 237ra266 (2014).
- Liu, Y. *et al.* A modified alpha-galactosyl ceramide for staining and stimulating natural killer T cells. *J. Immunol. Methods* **312**, 34–39 (2006).
- Geissmann, F. *et al.* Intravascular immune surveillance by CXCR6⁺ NKT cells patrolling liver sinusoids. *PLoS Biol.* **3**, e113 (2005).
- Harley, I. T. *et al.* IL-17 signaling accelerates the progression of nonalcoholic fatty liver disease in mice. *Hepatology* **59**, 1830–1839 (2014).
- Ivanov, I. I. *et al.* Specific microbiota direct the differentiation of IL-17-producing T-helper cells in the mucosa of the small intestine. *Cell Host Microbe* **4**, 337–349 (2008).
- Naik, S. *et al.* Compartmentalized control of skin immunity by resident commensals. *Science* **337**, 1115–1119 (2012).
- Chien, Y. H., Meyer, C. & Bonneville, M. gammadelta T cells: first line of defense and beyond. *Annu. Rev. Immunol.* **32**, 121–155 (2014).
- Cheng, M. *et al.* Microbiota modulate tumoral immune surveillance in lung through a gammadeltaT17 immune cell-dependent mechanism. *Cancer Res.* **74**, 4030–4041 (2014).
- Gray, E. E., Suzuki, K. & Cyster, J. G. Cutting edge: Identification of a motile IL-17-producing gammadelta T cell population in the dermis. *J. Immunol.* **186**, 6091–6095 (2011).
- Lee, J. S. *et al.* Interleukin-23-independent IL-17 production regulates intestinal epithelial permeability. *Immunity* **43**, 727–738 (2015).
- Belkaid, Y. & Naik, S. Compartmentalized and systemic control of tissue immunity by commensals. *Nat. Immunol.* **14**, 646–653 (2013).
- Chien, Y. H., Zeng, X. & Prinz, I. The natural and the inducible: interleukin (IL)-17-producing gammadelta T cells. *Trends Immunol* **34**, 151–154 (2013).
- Zeng, X. *et al.* gammadelta T cells recognize a microbial encoded B cell antigen to initiate a rapid antigen-specific interleukin-17 response. *Immunity* **37**, 524–534 (2012).
- Zeng, X. *et al.* Gamma delta T cells recognize haptens and mount a hapten-specific response. *Elife* **3**, e03609 (2014).
- Dieude, M. *et al.* Cardiolipin binds to CD1d and stimulates CD1d-restricted gammadelta T cells in the normal murine repertoire. *J. Immunol.* **186**, 4771–4781 (2011).
- Uldrich, A. P. *et al.* CD1d-lipid antigen recognition by the gammadelta TCR. *Nat. Immunol.* **14**, 1137–1145 (2013).
- Luoma, A. M. *et al.* Crystal structure of Vdelta1 T cell receptor in complex with CD1d-sulfatide shows MHC-like recognition of a self-lipid by human gammadelta T cells. *Immunity* **39**, 1032–1042 (2013).
- Russano, A. M. *et al.* Recognition of pollen-derived phosphatidyl-ethanolamine by human CD1d-restricted gamma delta T cells. *J. Allergy Clin. Immunol.* **117**, 1178–1184 (2006).
- Gumperz, J. E. *et al.* Murine CD1d-restricted T cell recognition of cellular lipids. *Immunity* **12**, 211–221 (2000).
- De Libero, G. & Mori, L. Recognition of lipid antigens by T cells. *Nat. Rev. Immunol.* **5**, 485–496 (2005).
- Born, W. K. *et al.* Hybridomas expressing $\gamma\delta$ T-cell receptors respond to cardiolipin and β 2-glycoprotein 1 (Apolipoprotein H). *Scand. J. Immunol.* **58**, 374–381 (2003).
- Rivera, C. A. *et al.* Toll-like receptor-4 signaling and Kupffer cells play pivotal roles in the pathogenesis of non-alcoholic steatohepatitis. *J. Hepatol.* **47**, 571–579 (2007).
- Zhan, Y. T. & An, W. Roles of liver innate immune cells in nonalcoholic fatty liver disease. *World J. Gastroenterol.* **16**, 4652–4660 (2010).
- Tajiri, K. & Shimizu, Y. Role of NKT Cells in the Pathogenesis of NAFLD. *Int. J. Hepatol.* **2012**, 850836 (2012).
- Nati, M. *et al.* The role of immune cells in metabolism-related liver inflammation and development of non-alcoholic steatohepatitis (NASH). *Rev. Endocr. Metab. Disord.* **17**, 29–39 (2016).
- Schnabl, B. & Brenner, D. A. Interactions between the intestinal microbiome and liver diseases. *Gastroenterology* **146**, 1513–1524 (2014).
- Quigley, E. M. & Monsour, H. P. The Gut microbiota and nonalcoholic fatty liver disease. *Semin. Liver. Dis.* **35**, 262–269 (2015).
- Wieland, A., Frank, D. N., Harnke, B. & Bambha, K. Systematic review: microbial dysbiosis and nonalcoholic fatty liver disease. *Aliment. Pharmacol. Ther.* **42**, 1051–1063 (2015).
- Joyce, S. A. *et al.* Regulation of host weight gain and lipid metabolism by bacterial bile acid modification in the gut. *Proc. Natl Acad. Sci. USA* **111**, 7421–7426 (2014).
- Mehta, P., Nuotio-Antar, A. M. & Smith, C. W. gammadelta T cells promote inflammation and insulin resistance during high fat diet-induced obesity in mice. *J. Leukoc. Biol.* **97**, 121–134 (2015).
- Byrne, C. D. & Targher, G. NAFLD: a multisystem disease. *J. Hepatol.* **62**, S47–S64 (2015).

53. Young, A. J., Marston, W. L. & Dudler, L. Subset-specific regulation of the lymphatic exit of recirculating lymphocytes *in vivo*. *J. Immunol.* **165**, 3168–3174 (2000).
54. Kenna, T. *et al.* Distinct subpopulations of gamma delta T cells are present in normal and tumor-bearing human liver. *Clin. Immunol.* **113**, 56–63 (2004).
55. Mangan, B. A. *et al.* Cutting edge: CD1d restriction and Th1/Th2/Th17 cytokine secretion by human Vdelta3 T cells. *J. Immunol.* **191**, 30–34 (2013).
56. Gomez de Agüero, M. *et al.* The maternal microbiota drives early postnatal innate immune development. *Science* **351**, 1296–1302 (2016).
57. Liu, K. *et al.* Origin of dendritic cells in peripheral lymphoid organs of mice. *Nat. Immunol.* **8**, 578–583 (2007).
58. Wang, J. *et al.* Lung natural killer cells in mice: phenotype and response to respiratory infection. *Immunology* **137**, 37–47 (2012).
59. Chen, Y. *et al.* Increased susceptibility to liver injury in hepatitis B virus transgenic mice involves NKG2D-ligand interaction and natural killer cells. *Hepatology* **46**, 706–715 (2007).

Acknowledgements

This work was supported by the Ministry of Science & Technology of China (973 Basic Science Project 2013CB944902, 2013CB530506), the Natural Science Foundation of China (#81401366, #91429303, #31230025), a General Financial Grant from the China Postdoctoral Science Foundation (2014M550351) and a Special Financial Grant from the China Postdoctoral Science Foundation (2015T80661). We thank the National Institutes of Health Tetramer Core Facility for providing the CD1d tetramers.

Author contributions

F.L. designed and performed most of the experiments and wrote the manuscript; X.H. and Y.C. designed and performed some of the experiments; L.B., X.G. and Z.L. designed the experiments and supplied important mouse model; H.W. and R.S. designed and

supervised the experiment, and revised the manuscript; and Z.T. provided the study strategy, designed and supervised the experiments, wrote the manuscript and financially supported the study.

Additional information

Supplementary Information accompanies this paper at <http://www.nature.com/naturecommunications>

Competing financial interests: The authors declare no competing financial interests.

Reprints and permission information is available online at <http://npg.nature.com/reprintsandpermissions/>

How to cite this article: Li, F. *et al.* The microbiota maintain homeostasis of liver-resident $\gamma\delta$ T-17 cells in a lipid antigen/CD1d-dependent manner. *Nat. Commun.* **8**, 13839 doi: 10.1038/ncomms13839 (2017).

Publisher's note: Springer Nature remains neutral with regard to jurisdictional claims in published maps and institutional affiliations.



This work is licensed under a Creative Commons Attribution 4.0 International License. The images or other third party material in this article are included in the article's Creative Commons license, unless indicated otherwise in the credit line; if the material is not included under the Creative Commons license, users will need to obtain permission from the license holder to reproduce the material. To view a copy of this license, visit <http://creativecommons.org/licenses/by/4.0/>

© The Author(s) 2017

Erratum: The microbiota maintain homeostasis of liver-resident $\gamma\delta$ T-17 cells in a lipid antigen/CD1d-dependent manner

Fenglei Li, Xiaolei Hao, Yongyan Chen, Li Bai, Xiang Gao, Zhexiong Lian, Haiming Wei, Rui Sun & Zhigang Tian

Nature Communications 8:13839 doi: 10.1038/ncomms13839 (2017); Published 9 Jan 2017; Updated 6 Apr 2017

The HTML version of this Article previously published had an incorrect volume number of 7; it should have been 8. This has now been corrected in the HTML; the PDF version of the paper was correct from the time of publication.



This work is licensed under a Creative Commons Attribution 4.0 International License. The images or other third party material in this article are included in the article's Creative Commons license, unless indicated otherwise in the credit line; if the material is not included under the Creative Commons license, users will need to obtain permission from the license holder to reproduce the material. To view a copy of this license, visit <http://creativecommons.org/licenses/by/4.0/>

© The Author(s) 2017